Molecular Psychiatry (2017) 22, 874–883

www.nature.com/mp

OPEN

ORIGINAL ARTICLE

Functional screening of Alzheimer risk loci identifies *PTK2B* as an *in vivo* modulator and early marker of Tau pathology

P Dourlen[1,2,3], FJ Fernandez-Gomez[4,5,6], C Dupont[1,2,3], B Grenier-Boley[1,2,3], C Bellenguez[1,2,3], H Obriot[4,5,6], R Caillierez[4,5,6], Y Sottejeau[1,2,3], J Chapuis[1,2,3], A Bretteville[1,2,3], F Abdelfettah[1,2,3], C Delay[1,2,3], N Malmanche[1,2,3], H Soininen[7], M Hiltunen[7,8], M-C Galas[4,5,6], P Amouyel[1,2,3,9], N Sergeant[4,5,6], L Buée[4,5,6], J-C Lambert[1,2,3,11] and B Dermaut[1,2,3,10,11]

A recent genome-wide association meta-analysis for Alzheimer's disease (AD) identified 19 risk loci (in addition to *APOE*) in which the functional genes are unknown. Using *Drosophila*, we screened 296 constructs targeting orthologs of 54 candidate risk genes within these loci for their ability to modify Tau neurotoxicity by quantifying the size of >6000 eyes. Besides *Drosophila Amph* (ortholog of *BIN1*), which we previously implicated in Tau pathology, we identified *p130CAS* (*CASS4*), *Eph* (*EPHA1*), *Fak* (*PTK2B*) and *Rab3-GEF* (*MADD*) as Tau toxicity modulators. Of these, the focal adhesion kinase *Fak* behaved as a strong Tau toxicity suppressor in both the eye and an independent focal adhesion-related wing blister assay. Accordingly, the human Tau and PTK2B proteins biochemically interacted *in vitro* and PTK2B co-localized with hyperphosphorylated and oligomeric Tau in progressive pathological stages in the brains of AD patients and transgenic Tau mice. These data indicate that *PTK2B* acts as an early marker and *in vivo* modulator of Tau toxicity.

Molecular Psychiatry (2017) **22,** 874–883; doi:10.1038/mp.2016.59; published online 26 April 2016

INTRODUCTION

Since 2009, the Alzheimer's disease (AD) genetic field has benefited from the advent of genome-wide association studies (GWASs), which revealed numerous genetic risk factors of AD. The International Genomics of Alzheimer's Project (IGAP) consortium was the latest attempt to improve our knowledge of the genetic landscape of AD by meta-analyzing the available GWAS for common late-onset AD. This study raised the number of genome-wide significant AD risk loci up to 19 in addition to *APOE*.[1]

However, while GWASs and IGAP in particular represent major breakthroughs in our understanding of the genetic risk underlying late-onset AD, it is difficult to identify the functional genes and variants within these loci and to understand how they mechanistically contribute to AD pathogenesis. These points are important challenges of the post-GWAS era, and strong efforts are needed to decipher the link between AD genetics and pathogenesis. To date, several studies have indicated that some of these genes, for example, *SORL1* or *ABCA7*, might be involved in amyloid precursor protein metabolism, Aβ peptide production or clearance,[2–4] implying that the amyloid cascade hypothesis could be relevant not only in monogenic forms of AD.[5] However, beyond the central role of amyloid precursor protein metabolism and its catabolites, we also recently described *BIN1* as the first genetic risk factor modulating Tau pathology.[6] This implies that pathological pathways directly involving Tau might also be responsible for the development of AD at the early stage. Interestingly, this latter point was reinforced by a recent report from IGAP describing a novel risk locus located near the gene encoding the Tau protein (*MAPT*) in non *APOE-ε4* carriers.[7] Within this background, one can argue that, in addition to *BIN1*, some of the recently discovered genetic risk factors of AD might exert their pathogenic effect by modulating toxicity of the Tau protein and/or neurofibrillary tangle (NFT) pathology.

For our study on *BIN1*,[6] we took advantage of the *Drosophila* model, which is a small model organism that displays easily scorable and AD-relevant readouts for high-throughput genetic modifier screens.[8] In *Drosophila*, expression of the human *MAPT* gene in the eye results in small rough eyes associated with vacuolar neurodegeneration without NFT formation.[9] It thus constitutes a genetically sensitized system of early-stage pre-NFT AD that allows the identification of genetic modifiers by assessing roughening and size of the eye as readouts of Tau neurotoxicity. In the present study, we decided to screen genes within AD risk loci in a systematic manner for their ability to modify Tau toxicity in flies.

MATERIALS AND METHODS

Drosophila genetics and imaging

Flies were raised at 25 °C on standard fly medium (Nutri-fly BF, Genesee Scientific, San Diego, CA, USA). We used the same GMR>Tau (2N4R) line as previously described.[6] RNA interference (RNAi) stocks were obtained from the National Institute of Genetics Fly Stock Center (NIG collection, Kyoto, Japan), the Vienna *Drosophila* RNAi Center (VDRC, GD and KK collections, Vienna, Austria) and the Harvard Transgenic RNAi project (TRiP, attP2 and attP40 collections). Additional loss-of-function mutant lines and gain-of-function lines were obtained from the Bloomington *Drosophila* Stock Center (BDSC, Bloomington, IN, USA) and the fly research community

[1]Institut Pasteur de Lille, Lille, France; [2]INSERM, UMR 1167, Lille, France; [3]Université de Lille, Lille, France; [4]INSERM, UMR-S 1172, Alzheimer and Tauopathies, Lille, France; [5]Univ. Lille, JPArc, Lille, France; [6]CHRU, Memory Clinic, Lille, France; [7]Institute of Clinical Medicine—Neurology and Department of Neurology, University of Eastern Finland and Kuopio University Hospital, Kuopio, Finland; [8]Institute of Biomedicine, University of Eastern Finland, Kuopio, Finland; [9]Centre Hospitalier Régional Universitaire de Lille, Lille, France and [10]Center for Medical Genetics, Ghent University Hospital, Ghent, Belgium. Correspondence: Dr P Dourlen, Dr J-C Lambert or Professor B Dermaut, Unité d'Epidémiologie et de Santé Publique—INSERM U 1167, Institut Pasteur de Lille, BP 245, Lille 59019, France.
E-mail: pierre.dourlen@pasteur-lille.fr or jean-charles.lambert@pasteur-lille.fr or bart.dermaut@pasteur-lille.fr
[11]These two authors are co-last authors.
Received 17 September 2015; revised 12 December 2015; accepted 20 January 2016; published online 26 April 2016

(Supplementary Table S2). For eye size measurement, we stuck fly heads on a 45°-angled piece of wood such that the left eye pointed to the top. We took images of the eyes with a Leica (Wetzlar, Germany) Z16 APO macroscope (>6000 images). We quantified the size of the eyes using Fiji software (open source, http://fiji.sc/). A detailed explanation of the screening in the eye is available in Supplementary Information. For results other than the ones of the screen, comparison of the eye size was performed by a Kruskal–Wallis test followed by Wilcoxon comparisons of the conditions of interest using R software. For wing imaging, we dissected and mounted *Drosophila* wings between a slide and a coverslip in vaseline oil. Images were taken with an AxioImager Z1 (Zeiss, Oberkochen, Germany) equipped with a ×2.5 objective. Proportions of flies with blisters on 0, 1 or 2 wings were compared with a Cochran–Mantel–Haenszel test using R software over three experiments.

Transcriptional analysis

See Supplementary Information.

Immunohistofluorescence of human and mouse brain tissue

Formalin-fixed brain tissue samples were obtained from hippocampus and frontal cortex of eight neuropathologically confirmed AD patients at Braak stages II–VI (Supplementary Table S4). Human brain samples were obtained from the Lille Neurobank, which was given to the French Research Ministry by the Lille Regional Hospital (CHRU-Lille) on 14 August 2008 under the reference DC-2000-642. The Lille Neurobank fulfills criteria from the French Law on biological resources, including informed consent, ethics review committee and data protection (article L1243-4 of the Code de la Santé publique, August 2007). THY-Tau22 transgenic mice (five animals per age) were killed by decapitation and the brains were rapidly recovered and postfixed for 7 days in phosphate-buffered saline (PBS) with 4% paraformaldehyde. The postfixed brains were kept at 4 °C in 30% sucrose in PBS until inclusion in Tissue Tek. Floating sections (40-µm thick) of human and mouse brain were performed with a Leica CM3050 cryostat microtome. Slices were immersed in PBS-0.2% Triton and blocked with goat/horse serum (Vector Laboratories, Burlingame, CA, USA) for 60 min. Slices were incubated overnight at 4 °C with AT8 (phosphoSer202-phosphoThr205 Tau, MN1020 Thermo Fisher Scientific, Waltham, MA, USA) or TOC1 (antibody against Tau oligomers, generous gift of Pr. LI Binder) and PTK2B (SAB4300468, Sigma-Aldrich, Saint-Quentin Fallavier, France) antibodies diluted in PBS with 0.2% Triton. After several washes in PBS-0.2% Triton, brain slices were incubated 60 min at room temperature with Alexa Fluor 488 and 568 goat secondary anti-rabbit and anti-mouse antibodies in PBS-0.2% Triton. After several PBS washes, autofluorescence was quenched by incubating the brain slices with a Sudan Black solution according to the manufacturer's instructions (Merck Millipore, Darmstadt, Germany). Slices were mounted under a coverslip with Vectashield mounting medium for fluorescence with 4,6-diamidino-2-phenylindole (Vector Laboratories, AbCys). Images were acquired with a Zeiss Apotome and a Zeiss confocal LSM710 microscope for human and mouse brain images, respectively.

GST pull down

GST-PTK2B construct was generated by synthesizing the PTK2B sequence in between BamH1/XhoI sites (geneart, Thermo Fisher Scientific) and subcloning the sequence into PGEX 6P1 plasmid (GE Healthcare Life Sciences, Buckinghamshire, England). HEK293 cells were transfected with pCMV-SPORT6-PTK2B (IMAGE ID: 4343040) to overexpress PTK2B. Tau-expressing plasmid and GST-Tau constructs are published.[10] Details about the protocol are available in Supplementary Information. Proteins were detected by immunoblot using PTK2B antibody (P3209, Sigma-Aldrich) and chemiluminescence.

Western blotting analysis

Drosophila heads were dissected and crushed in LDS sample buffer supplemented with antioxidant (Life Technologies) and analyzed by sodium dodecyl sulfate-polyacrylamide gel electrophoresis (4–12% gel NuPAGE Novex, Life Technologies). Proteins were detected by immunoblot using AT8 (phosphoSer202-phosphoThr205 Tau, MN1020 Thermo-Pierce), phosphoTyr18 Tau (MM-0194-100, MediMabs, Montréal, Québec, Canada), RZ3 (phosphoThr231, Dr P Davies), PHF1 (phosphoSer396 phosphoSer404, Dr P Davies), Tau1 (dephosphorylated aa197-205, MAB3420, Millipore), AT270 (phosphoThr181, MN1050, Thermo-Pierce), pS422 (phosphoSer422, 44764G, Life Technologies) and actin (A2066, Sigma-Aldrich) antibodies and chemiluminescence.

RESULTS

Selection of *Drosophila* orthologs of candidate AD risk genes

We selected all annotated genes within the 19 IGAP genomic risk regions (with the exception of the *APOE* locus) as defined by IGAP regional association plots assuming that the functional risk variants are located in the vicinity of the single-nucleotide polymorphism (SNP) producing the top signal and taking into account the linkage disequilibrium patterns within the loci of interest (Supplementary Table S1). We identified 148 human genes within these intervals and determined their corresponding *Drosophila* orthologs with the *Drosophila* RNAi Screening Center Integrative Ortholog Prediction Tool (DIOPT; http://www.flyrnai.org/diopt).[11] We used a DIOPT cutoff score of ⩾3 to select high confidence homologs.[11] We found that 54 of the 148 human genes had at least one *Drosophila* ortholog. From the 19 loci, 6 were excluded for further analysis (31%), because they did not contain any fly orthologs in the genomic region of interest (*CR1*, *CLU*, *HLA-DRA*, *MS4A6A*, *NME8*, *SORL1*). Conversely, some human genes had several *Drosophila* orthologs and we retained 74 *Drosophila* orthologs corresponding to 54 human genes in the 13 remaining loci (Supplementary Figure S1; Supplementary Table S1). For these 74 orthologs, we obtained 274 corresponding RNAi lines, that is, around 4 RNAi lines per gene of interest, from 5 publicly available collections (Supplementary Figure S1; Supplementary Table S2).

Genetic screen of candidate AD risk genes identifies *BIN1* and four novel modifiers of Tau toxicity

To test whether these *Drosophila* orthologs could modify Tau neurotoxicity, RNAi lines were crossbred with flies expressing the longest isoform of human Tau (2N4R) in the eye (*GMR* driver). In this model, expression of Tau causes neuronal degeneration without NFT formation and results in smaller rough eyes.[12,13] We determined whether RNAi-mediated knockdown of the genes of interest were able to modify this Tau-induced phenotype by quantifying the eye surface (Figure 1a). We discarded all RNAi lines

Figure 1. Functional screen of AD susceptibility loci in *Drosophila*. (**a**) Quantification of the eye size of flies co-expressing Tau and AD candidate gene loss-/gain-of-function constructs. Each symbol in the graph represents the median of the measurement of the size of 10 fly eyes per construct and control (30 values for the 3 pooled controls). Blue circles, squares and triangles represent RNAi, mutant and overexpression constructs, respectively (○, □, Δ), and black circles represent controls (○). For RNAi, we plotted values normalized according to their origin (see Materials and Methods section). When the size of the eye was statistically different from the control (Wilcoxon test, Bonferroni correction, for RNAi with and without correction), we used red color (○, □, Δ). Positive hits were re-tested and plotted with filled symbols (●, ■, ▲, ●, ■, ▲). The two horizontal lines mark the eye size range of the Tau expressing control. Constructs that are above the controls are Tau toxicity suppressors and the ones that are lower are enhancers. Vertical dashed and solid lines separate *Drosophila* genes and loci. The name of the *Drosophila* gene targeted by the construct is indicated below the two graphs, as well as the name of their human orthologs and the name of the locus they belong to. Positive hits are shaded in gray. (**b**) Representative images of the positive hits (scale bar 0.1 mm). Images for the *Fak* gene are available in Figure 2.

that induced an external eye phenotype on their own when expressed with the *GMR* driver. Heterozygous genomic loss-of-function alleles and overexpression constructs were also tested when available. Genes were considered positive hits when at least two lines (RNAi, mutant alleles or overexpressing constructs) from different collections modified Tau toxicity (Figure 1a;

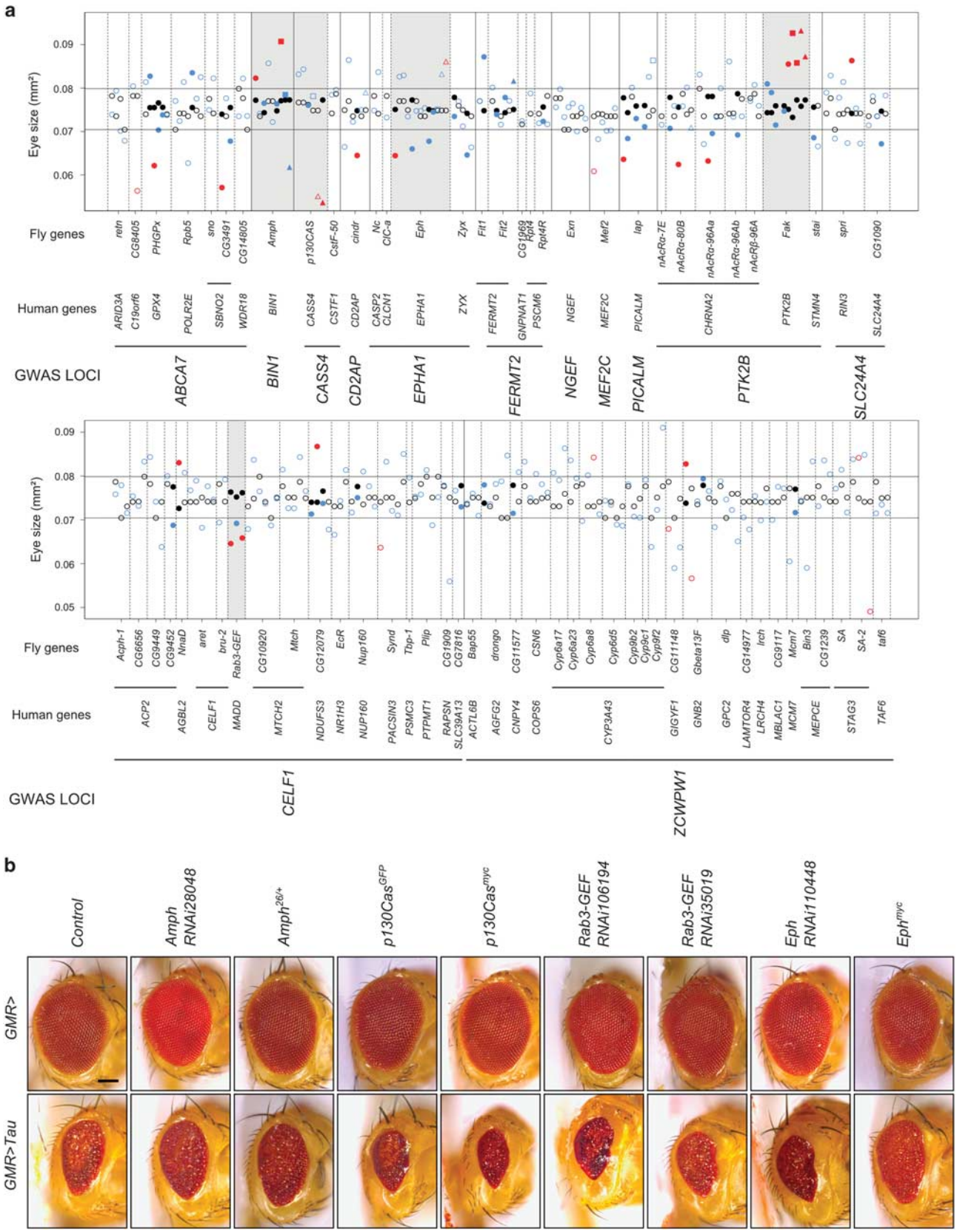

Figure 1. For caption please refer page 875.

Supplementary Table S3; Table 1). RNAi and mutant alleles had to give identical suppressing or enhancing effects.

By applying these criteria, we confirmed that *BIN1* ortholog *Amph* modulates Tau toxicity (Figures 1a and b; Supplementary Table S3; Table 1) as we previously reported.[6] In addition, we identified the *Drosophila* genes *p130CAS* (ortholog of *CASS4*), *Eph* (ortholog of *EPHA1*), focal adhesion kinase (*Fak*; ortholog of *PTK2B*) and *Rab3-GEF* (ortholog of *MADD*) (Figures 1a and b; Supplementary Table S3; Table 1) as Tau toxicity modulators. Although downregulation of *Eph* and *Rab3-GEF*, and upregulation of *p130CAS*, enhanced Tau toxicity, both upregulation and downregulation of *Fak* suppressed Tau toxicity (Figures 1a and b; Supplementary Table S3; Table 1). Of note, *p130Cas*, *Eph* and *Fak* correspond to orthologs of genes closest to the top SNP signal in the IGAP study, while this is not the case for *Rab3-GEF* for which the top GWAS signal was within the *CELF1* gene (Supplementary Figure S2).

PTK2B ortholog *Fak* suppresses Tau toxicity in the eyes and wings

We focused on the *PTK2B* ortholog *Fak*, as it behaved as a consistent suppressor of Tau toxicity in our screen suggesting that *Fak* might be a specific downstream mediator of Tau toxicity (Figures 2a and b). We confirmed the Tau–*Fak* genetic interaction in the eye with an independent 0N4R Tau construct, the Fak^{CG1} null[14] and the Fak^{KG} hypomorphic[15] alleles in heterozygous, homozygous and transheterozygous states. The transheterozygous genotype is important to rule out effects of possible second-site mutations on the chromosome. The 0N4R Tau construct allows assessing the requirement of the 2 N alternative domains of Tau for the interaction. We also observed a *Fak* gene dose-dependent suppression of Tau toxicity, confirming the Tau–*Fak* interaction without requirement of the 2 N domains of Tau (Figures 2c and d). Next we wanted to confirm the interaction between *Fak* and Tau in an independent assay and chose the more specific wing blister phenotype, which links *Fak* to its established function in the focal adhesion pathway downstream of integrins.[16] Wing blisters are the result of cell adhesion defects between the dorsal and ventral blade of the wing. As reported previously,[16] overexpression of *Fak* results in wing blisters in 20% of the flies (Supplementary Figure S3). We tested the expression of Tau (2N4R) in the posterior compartment of the wing using the *engrailed* driver. Overall, 62% and 11% of the flies exhibited blisters in one or their two wings, respectively, in addition to a reduced wing size (Figures 2e and f). When co-expressed with *Fak* RNAi, the proportion of flies with wing blisters in one or two wings significantly decreased to 53% and 2%, respectively. With this readout, we also wanted to confirm the interaction with an independent Tau construct and *Fak* loss-of-function mutations. We used the Tau construct expressing the 0N4R Tau isoform. Expression of this construct induced a strong reduction of the wing size with some of them exhibiting blisters (Supplementary Figure S4). In $Fak^{CG1/+}$ and $Fak^{KG/+}$ loss-of-function backgrounds, the size of the posterior compartment of the wing was partially restored but we were unable to quantify the blister frequency owing to the greatly reduced wing size (Supplementary Figure S4). To circumvent this problem, we tested the phosphodeficient Tau^{AP} (0N4R) construct, in which 14 Serine or Threonine phosphorylation sites are mutated into alanine and which is known to be less toxic in the eye.[17] Expression of Tau^{AP} was also less toxic in the wing and resulted in a mild reduction of the wing size, with 80% of the flies exhibiting typical blisters in their two wings (Figures 2g and h). In $Fak^{CG1/+}$ and $Fak^{KG/+}$ backgrounds, the proportion of flies with blisters in their two wings was significantly reduced to 31% and 62%, respectively. Together, using three different *Fak* and three different Tau lines, these results indicated that *Fak* and Tau genetically interact in an independent readout related to focal adhesion.

Table 1. Summary of the functional screen results of the AD risk loci in *Drosophila*

IGAP locus	*Human genes (with fly orthologs)*	*Fly genes*	*Tau-toxicity modifiers (human ortholog)*
CD2AP	3 (1)	1	
BIN1	1 (1)	1	*Amph (BIN1)*
MEF2C	4 (1)	1	
PICALM	2 (1)	1	
INPP5D	3 (1)	1	
SLC24A4	2 (2)	2	
CASS4	6 (2)	2	*p130CAS (CASS4)*
FERMT2	6 (4)	6	
EPHA1	10 (4)	4	*Eph (EPHA1)*
PTK2B	5 (3)	7	*Fak (PTK2B)*
ABCA7	12 (6)	7	
CELF1	23 (13)	18	*Rab3-GEF (MADD)*
ZCWPW1	46 (15)	23	
Total	123 (54)	74	

Abbreviations: AD, Alzheimer's disease; IGAP, International Genomics of Alzheimer's Project.

PTK2B and Tau interact biochemically *in vitro*

We next tested whether PTK2B and Tau are able to physically interact. We performed GST pull down experiments (Figures 3a and b). We were able to pull down PTK2B from PTK2B-transfected HEK293 cell extracts with GST-Tau1N4R and GST-Tau2N4R constructs (Figure 3a). Reciprocally, we were able to pull down 1N4R and 2N4R Tau isoforms from transfected HEK293 cell extracts with a GST-PTK2B construct (Figure 3b). These results indicate that PTK2B and Tau interact directly or indirectly in a complex.

As PTK2B is a protein tyrosine kinase, we tested whether PTK2B could phosphorylate Tau directly or indirectly through the activation of other kinases. 2N4R Tau isoform has five tyrosine residues (Tyr18, Tyr29, Tyr197, Tyr310, Tyr394) but antibodies have been developed only for Tyr18. In *Drosophila*, we assessed the effect of the modulation of Fak on the phosphorylation of Tau Tyr18 and on the main AD Tau phosphorylation sites (Figure 3c).

Figure 2. Genetic interaction between *Fak*/*PTK2B* and Tau in the eye and wing of *Drosophila*. (**a**) Images of fly eyes expressing the 2N4R Tau isoform (*GMR>Tau*) in five different *Fak* conditions (scale bar 0.1 mm). The *GMR>* images are the five different *Fak* conditions without Tau expression as control. (**b**) Quantification of the eye size of the progeny of Tau-expressing flies crossed with the different lines targeting *Fak* ($*P < 1.68 \times 10^{-4}$). (**c**) Images of fly eyes expressing the 0N4R Tau isoform or the control *mCherryNLS* construct in the background expressing decreasing amount of *Fak*, from wild-type expression of *Fak* to no expression of *Fak* in $Fak^{CG1/CG1}$ flies (scale bar 0.1 mm). (**d**) Corresponding quantification of the eye size. (**e**) Wings co-expressing Tau (2N4R) or *GFP* and $Fak^{RNAi17957}$ or *GFP* with the *engrailed* driver. The dashed line in the top left panel marks the border between the anterior and posterior compartment, the driver being expressed in the latter (scale bar 0.5 mm). Arrows label wing blisters (yellow shaded). (**f**) Quantification of the wing phenotype in flies co-expressing Tau or GFP and $Fak^{RNAi17957}$ or GFP. The total numbers of flies over three experiments are indicated above the column. (**g**) Wings expressing GFP and Tau^{AP} (0N4R) with the *engrailed* driver in wild-type and $Fak^{+/-}$ backgrounds. Arrows label wing blisters (yellow shaded) (scale bar 0.5 mm). (**h**) Quantification of the wing phenotype in flies expressing GFP and Tau^{AP} in wild-type and $Fak^{+/-}$ backgrounds. The total numbers of flies over three experiments is indicated above the column.

Loss and gain of *Fak* did not change the phosphorylation of these sites. Of note, this is in agreement with the suppressive effect of *Fak* on the phosphodeficient Tau^{AP}-induced phenotypes in the wing (Figures 2g and h). As we cannot exclude that Fak modulates other tyrosine or non-tyrosine Tau phosphorylation sites directly or indirectly, we tested whether the kinase activity of Fak is required for the suppression of Tau toxicity. We tested a FakY430F mutant in which the Tyr430 autophosphorylation site is mutated

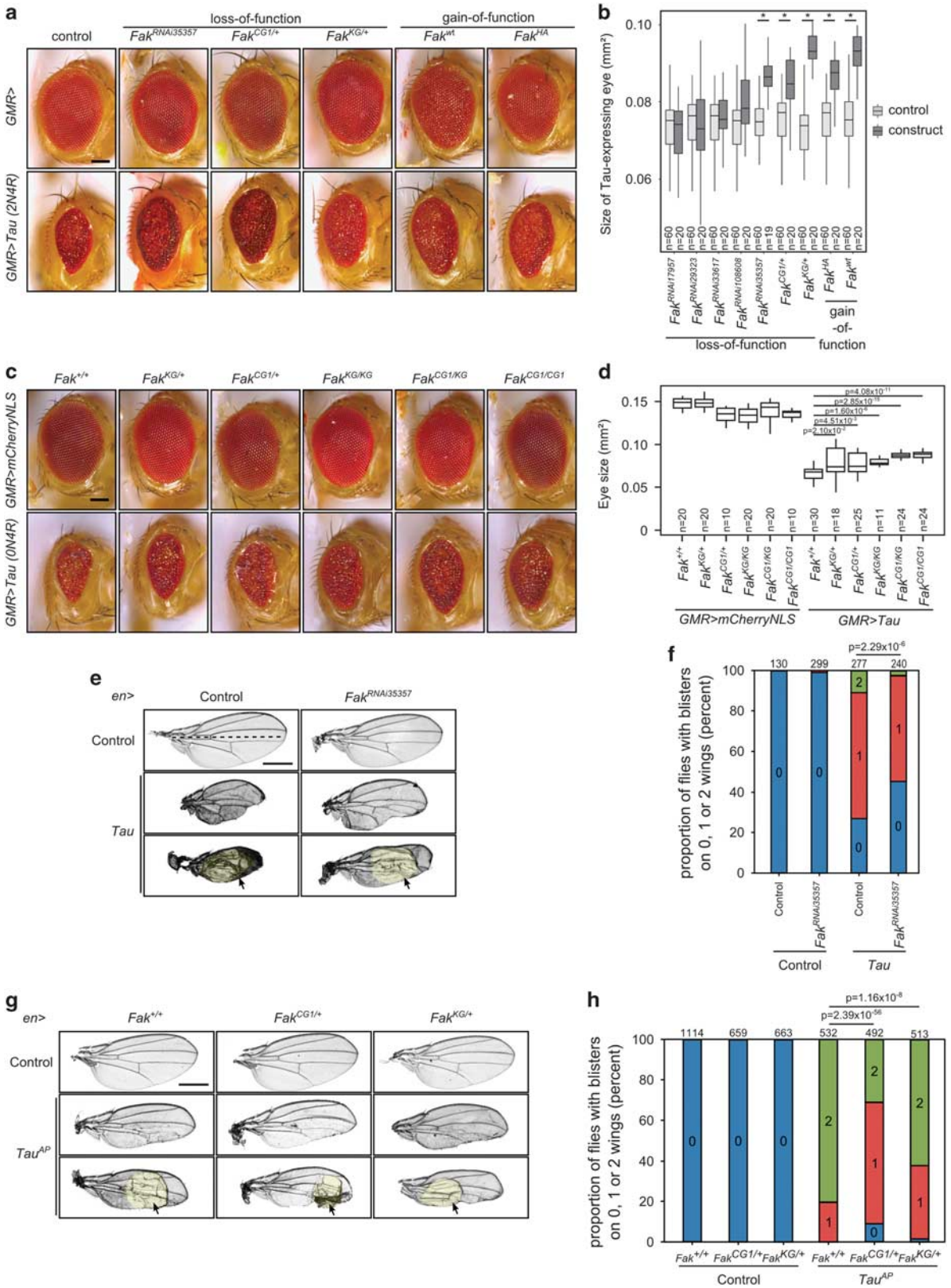

Figure 2. For caption please refer page 877.

into the non-phosphorylable Phe residue, a mutant that has been used as a mutant of Fak kinase activity.[15,18,19] We observed that FakY430F also suppressed Tau toxicity (Figure 3d). This suggested that the suppressive effect of Fak on Tau toxicity is independent of its kinase activity.

Neuronal cell bodies harboring hyperphosphorylated and oligomeric Tau accumulate PTK2B in the brains of AD patients and transgenic Tau mice

To further validate a potential link between PTK2B and Tau pathology, we assessed whether the mRNA levels of *PTK2B* in the

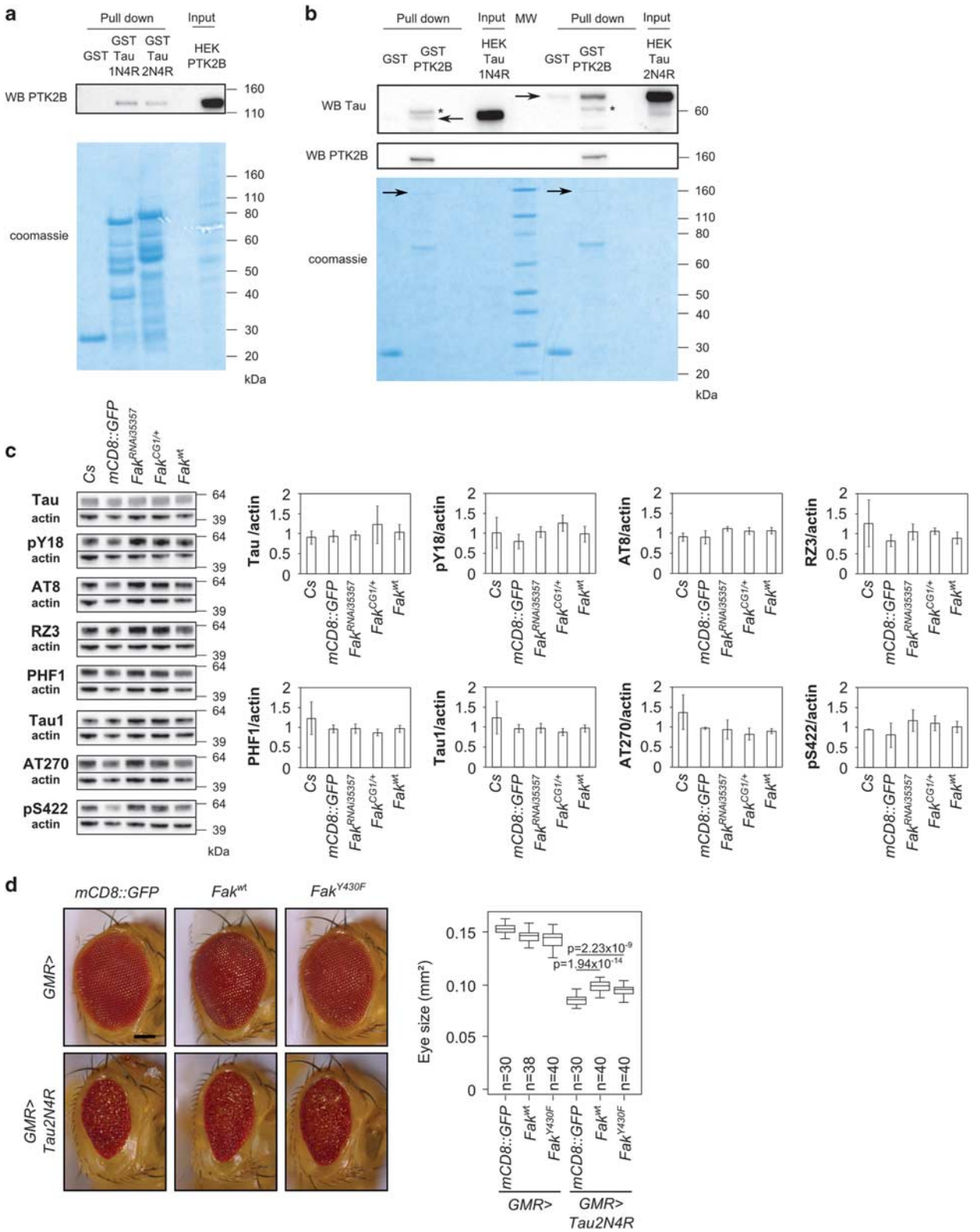

Figure 3. For caption please refer page 880.

temporal AD cortex were altered in relation to the progression of neurofibrillary pathology (Braak staging). No statistically significant differences between different Braak groups were observed (Supplementary Figures S5a and b). Next we co-labeled Tau and PTK2B in the human AD brains (Figure 4a). Already in early-stage AD brains (Braak stage II), PTK2B was clearly detectable in Tau-positive NFTs and neuritic processes labeled with the AT8 phospho-Tau antibody. In an advanced stage of AD (Braak stage VI), PTK2B staining was more abundant and overlapped strongly with AT8 indicating that PTK2B co-accumulates with NFTs (Figure 4a; Supplementary Table S4). To determine whether PTK2B accumulation occurs early during Tau pathology, we performed a co-staining for PTK2B and Tau oligomers detected with the TOC1 antibody.[20] We observed a colocalization between PTK2B and TOC1 staining, indicating that PTK2B accumulation is an early event in AD pathogenesis (Figure 4b). Accumulation of phosphorylated PTK2B has been observed in the brains of the Tau transgenic pR5 mouse model.[21] Using our THY-Tau22 mouse model showing hippocampal NFTs starting at 2–4 months,[22] we assessed the neuronal presence of PTK2B at 2, 5 and 13 months to establish whether PTK2B and Tau accumulate in the same neurons and whether this is an early or late event. Accumulation of PTK2B started at 2 months and progressively co-accumulated within the cytoplasm of a growing number of AT8-positive degenerating neurons (Figure 4c). These data suggest that the accumulation of PTK2B represents an early pathological marker tightly coinciding with progressive Tau pathology in AD.

DISCUSSION

In the postgenomic era, the identification of the causal genes and their pathogenic function within GWAS-defined genomic risk intervals for common diseases constitutes a major challenge. Indeed, most signals discovered by GWASs do not clearly define the responsible causal genes but typically implicate a broad genomic region containing a number of candidate genes. Experimental confirmation is therefore critical to validate a target for further mechanistic investigation. For AD, the IGAP consortium recently defined 19 risk regions containing around 150 candidate genes in addition to *APOE*. We here present, to the best of our knowledge, the first systematic functional *in vivo* follow-up study of IGAP AD risk loci and identified, next to *BIN1*, four novel Tau toxicity modulators. Among these, we observed strong interactions between Tau and focal adhesion gene *PTK2B* in the flies, mice and human AD brains, together suggesting that PTK2B is an important early marker and modulator of Tau pathology in AD.

A first important aim of our study was to identify causal genes in the 19 AD risk regions. To do so, we used the high-throughput *Drosophila* system to screen hundreds of constructs corresponding to IGAP AD candidate risk genes for their ability to modify the neuronal toxicity of Tau. We could study 13 of the 19 loci of interest (*ABCA7*, *BIN1*, *CASS4*, *CD2AP*, *CELF1*, *EPHA1*, *FERMT2*, *INPP5D*, *MEF2C*, *PICALM*, *PTK2B*, *SLC24A4* and *ZCWPW1*) because the genes of the remaining 6 loci (*CR1*, *HLA*, *NME8*, *CLU*, *MS4A6A*, *SORL1*) do not contain *Drosophila* orthologs with sufficient homology. Importantly, we followed a quantitative and well-controlled strategy that included the accurate measurement of eye size and applied strict gene selection criteria to restrict the number of false-positive or inconsistent results introduced by variability in culture conditions, genetic background, RNAi-mediated off-target effects and second-site mutations.

As a result, in addition to *BIN1*, we identified four new genes, *PTK2B*, *CASS4*, *EPHA1* and *MADD*, in four loci, as modifiers of Tau toxicity. *PTK2B*, *CASS4* and *EPHA1* are the closest genes to the top GWAS signal of their locus, whereas, in the *CELF1* locus, we identified the ortholog of *MADD* although the most significantly associated SNP lies in the *CELF1* gene. Of note, the *Drosophila aret* gene, ortholog of the *CELF1* gene, has been previously suggested to modify Tau toxicity in another *Drosophila* screen.[23] However, the screening approach was different from ours as it used a frontotemporal dementia-associated Tau construct (0N4R Tau^{V337M}), other gain- and loss-of-function lines and a qualitative rather than a quantitative way to assess Tau toxicity. The involvement of the four identified genes in AD is supported by literature data. SNPs within or adjacent to *EPHA1*, *PTK2B* and *CASS4* are associated with AD clinical progression.[24] When evaluating crosstalk between AD risk loci by protein quantitative trait analysis, rs2718058A, an AD susceptibility allele in the *NME8* locus, was associated with increased *PTK2B* expression.[25] In AD pathological conditions, a reduction in EPHA4 and EPHB2 receptor levels, belonging to the Eph receptor family such as EPHA1, has been found in postmortem hippocampal tissue from patients with incipient AD and in an AD mouse model overexpressing human amyloid-β protein precursor.[26] Finally, in AD brains and an Aβ cellular model, *MADD* expression is reduced and *MADD* splicing is altered, which promote neuronal vulnerability.[27,28] For the eight remaining loci (*ABCA7*, *CD2AP*, *FERMT2*, *INPP5D*, *MEF2C*, *PICALM*, *SLC24A4* and *ZCWPW1*), we did not identify positive hits. Beyond the fact that the causal genes of these loci may not affect Tau toxicity, it is important to keep in mind that some genes in these loci have *Drosophila* orthologs with a low homology score, which were not tested. This is the case for *ABCA7*, in which loss-of-function functional variants that confer risk of AD were recently discovered.[29] The novel genes we identified were previously not linked to Tau toxicity and suggest that a higher than expected number of risk genes act at the level of Tau rather than Aβ pathology. This notion is in accordance with recent work supporting the *MAPT* locus as a genetic risk factor for AD[7] and with the general central role of *MAPT* in a wide range of neurodegenerative diseases.[30] However, it is important to note that our functional screening strategy did not test for possible interactions with Aβ toxicity and it is equally well possible that some of the AD risk genes affect pathways that are not directly linked to Tau or Aβ.

As *Fak* appeared as a strong suppressor of Tau toxicity among our five genes of interest, we decided to further decipher its relation with Tau. First, we were able to validate the interaction of *Fak* with Tau toxicity in a focal adhesion-related wing blister assay that is fully independent of the Tau-related toxicity in eyes. Second, we observed an *in vitro* biochemical interaction between

Figure 3. *In vitro* biochemical interaction between PTK2B and Tau. (**a**) Pull down of PTK2B with GST, GST-Tau1N4R and GST-Tau2N4R protein constructs. Upper panel: detection of PTK2B in the pull down extract by western blotting. Lower panel: corresponding Coomassie blue gel used as loading control of GST constructs. (**b**) Pull down of Tau1N4R and Tau2N4R with GST and GST-PTK2B protein constructs. Upper panel: detection of Tau (arrows) in the pull down extract by western blotting (an unspecific band is labeled with a star, MW, molecular weight). Lower panel: corresponding Coomassie blue gel used as loading control of GST constructs. As the GST-PTK2B constructs were difficult to produce and visualize with Coomassie blue staining (arrows), we checked the GST-PTK2B construct through detection of PTK2B by western blotting (middle panel). All results shown in panels (**a** and **b**) are representative of three independent experiments. (**c**) Western blotting analysis of Tau phosphorylation in different *Fak* conditions in the *Drosophila* eye. Actin is used as a loading control ($n = 2–4$). (**d**) Images and quantification of fly eyes co-expressing the 2N4R Tau isoform and a *mCD8::GFP* construct used as control or wild-type *Fak* or mutant Fak^{Y430F} (scale bar 0.1 mm).

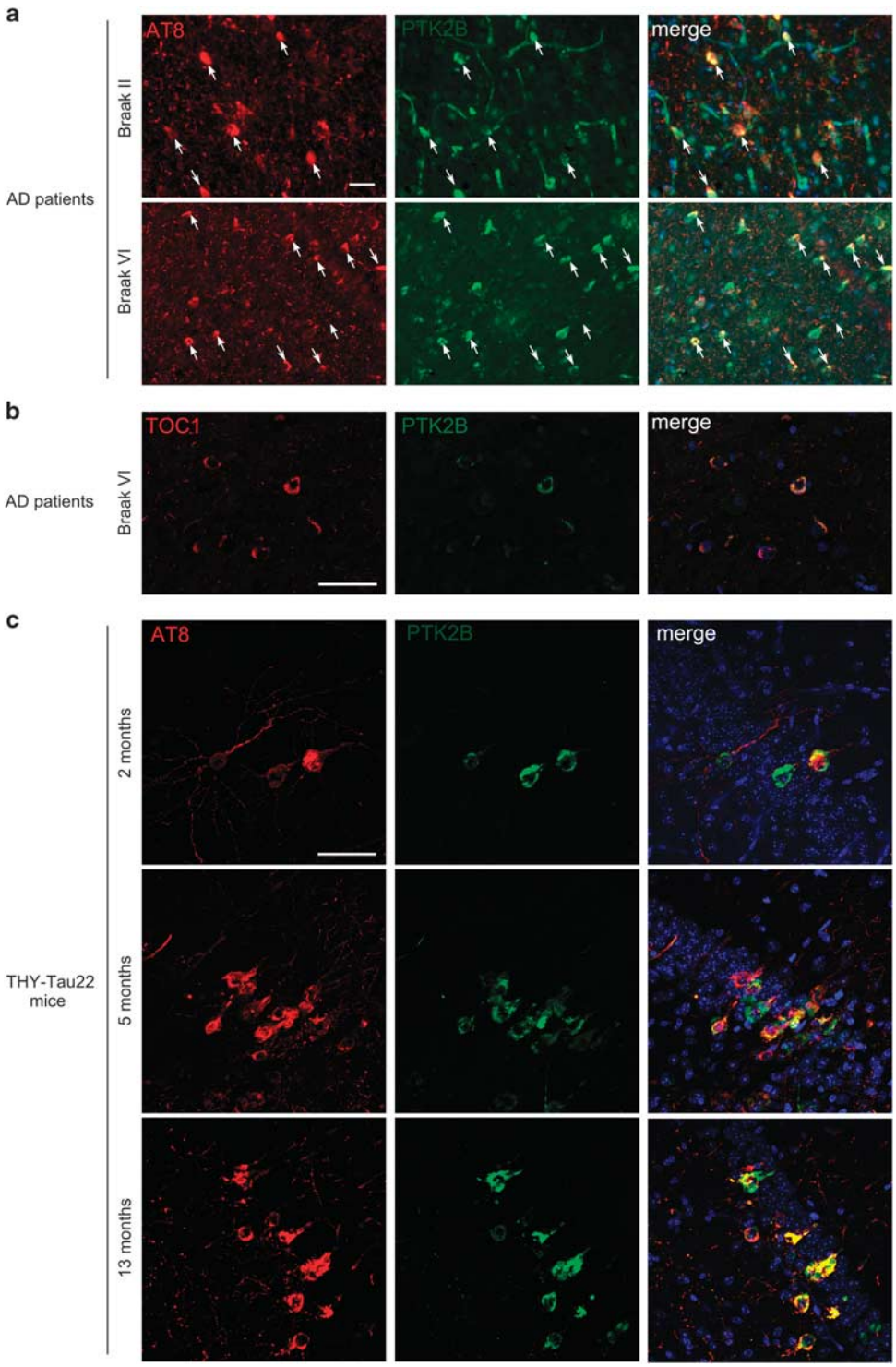

Figure 4. PTK2B colocalizes with neurofibrillary degeneration in the brains of AD patient and Tau transgenic mouse. Co-labeling of PTK2B with phospho-Tau (**a**) and PTK2B with oligomeric Tau (**b**) in the hippocampus of AD patients at Braak stages II and VI (scale bar 50 μm). (**c**) Co-labeling of PTK2B with phospho-Tau in the hippocampus CA1 region of 2-, 5- and 13-month-old THY-Tau22 transgenic mice (scale bar 50 μm). AD, Alzheimer's disease.

the human Tau, especially the 4R domain, and PTK2B proteins. Finally, PTK2B co-localized with hyperphosphorylated and oligomeric Tau in progressive pathological stages in the brains of AD patients and transgenic Tau mice. Altogether, these data strongly support PTK2B as a genetic risk factor of AD likely involved in the pathophysiological processes implicating Tau. In line with this hypothesis, the time course analysis of Tau pathology in the THY-Tau22 mouse model indicated that the accumulation of PTK2B occurred simultaneously with the appearance of the first AT8-positive labeling in neurons, and in the brain of AD patients, the accumulation of PTK2B occurred in neurons exhibiting Tau oligomers. This implies PTK2B as an actor of very early events in

Tau pathology. Of note, a redistribution of activated PTK2B to the perinuclear region of pyramidal neurons has been described in chronically stressed rats and is associated with retraction of dendritic arbors.[31] However, whether the accumulation of PTK2B in the soma of degenerating neurons is a cause or a consequence of Tau pathology remains to be explored.

Although the exact mechanism remains uncertain, it is interesting to note that three of our positive hits *Fak/PTK2B*, *p130CAS/CASS4* and *Eph/EPHA1* have previously been implicated in the focal adhesion pathway. PTK2B and CASS4, respectively, belong to the FAK and CAS families of proteins, which are known to directly interact in the cell adhesion pathway.[32,33] PTK2B has been reported to physically interact with members of the CAS family downstream of integrins.[34] The EPH receptor family is less directly connected. The activation of EPHA4, a paralog of EPHA1, inhibits β1 integrin downstream signaling pathways, including BCAR1 (a paralog of CASS4) and PTK2B, and regulates dendritic spine morphology in hippocampal pyramidal neurons.[35] Ephrin-A1 ligand induces carcinoma cell retraction through EPHA2, a paralog of EPHA1, and downstream SRC and FAK, a paralog of PTK2B.[36] Hence, our results suggest that a cell adhesion pathway based on PTK2B and CASS4, and possibly regulated by EPHA1, could be involved in Tau pathology and AD pathogenesis (Supplementary Figure S6). Accordingly, *Drosophila* screening of pre-IGAP AD risk genes also identified genes related to the focal adhesion pathway as modulators of Tau toxicity.[23] Of note, the cell adhesion pathway has already been involved in AD as a potent link between Aβ peptide and Tau pathogenesis.[37–39]

In conclusion, our work highlights the role of PTK2B as a major actor in AD pathogenesis at the level of Tau toxicity.

CONFLICT OF INTEREST

The authors declare no conflict of interest.

ACKNOWLEDGMENTS

We thank Dr GL Boulianne, Dr AC Zelhof, Dr F Roegiers, Dr EA Golemis, Dr AL Kolodkin, Dr JR Terman, Dr RL Cagan, Dr JB Thomas, Dr A Sehgal, Dr RH Palmer, Dr M Vidal, the Bloomington Drosophila Stock Center (NIH P40OD018537), the National Institute of Genetics Fly Stock Center, the Vienna Drosophila RNAi Center and the Harvard Transgenic RNAi project at Harvard Medical School (NIH/NIGMS R01-GM084947) for providing *Drosophila* stocks. We thank the BioImaging Center Lille-Nord de France (BICeL) platform. We thank MH Gevaert and RM Siminski (Laboratoire d'Histologie, Faculté de Médecine, Lille, France) for technical assistance. We express gratitude to Alzheimer's disease patients and their families who allowed us to perform brain autopsies. We thank Professor V Deramecourt, Dr P Gelé and the Lille NeuroBank for access to the patient brains. We thank the IGAP consortium for sharing results of the published GWAS. We thank Dr J Shulman for helpful discussions. This work was funded by the French National Fondation on Alzheimer's disease and related disorders, the EU FP7 project AgedBrainSYSBIO (Grant Agreement No. 305299), the French government's CPER-Neuroscience (DN2M) program (Nord-Pas de Calais Regional Council and FEDER), the Fondation pour la Recherche Médicale (ING20140129268), LECMA - Vaincre Alzheimer (grant 13755), the Lille Métropole Communauté urbaine council, Lille University, CNRS, Interuniversity Attraction Poles program P7/16 of the Belgian Science Policy Office (BELSPO), the LABEX (laboratory of excellence program investment for the future) DISTALZ grant (Development of Innovative Strategies for a Transdisciplinary approach to ALZheimer's disease), Alzheimer's association grant (BFG-14-318355) and the Academy of Finland, VTR grant V16001 of Kuopio University Hospital, Sigrid Jusélius Foundation, the Strategic Funding of the University of Eastern Finland (UEF-Brain), FP7, Grant Agreement No. 601055, VPH Dementia Research Enabled by IT VPH-DARE@IT.

REFERENCES

1 Lambert J-C, Ibrahim-Verbaas CA, Harold D, Naj AC, Sims R, Bellenguez C *et al.* Meta-analysis of 74,046 individuals identifies 11 new susceptibility loci for Alzheimer's disease. *Nat Genet* 2013; **45**: 1452–1458.
2 Rogaeva E, Meng Y, Lee JH, Gu Y, Kawarai T, Zou F *et al.* The neuronal sortilin-related receptor SORL1 is genetically associated with Alzheimer disease. *Nat Genet* 2007; **39**: 168–177.
3 Willnow TE, Andersen OM. Sorting receptor SORLA--a trafficking path to avoid Alzheimer disease. *J Cell Sci* 2013; **126**: 2751–2760.
4 Kim WS, Li H, Ruberu K, Chan S, Elliott DA, Low JK *et al.* Deletion of Abca7 increases cerebral amyloid-β accumulation in the J20 mouse model of Alzheimer's disease. *J Neurosci* 2013; **33**: 4387–4394.
5 Bohm C, Chen F, Sevalle J, Qamar S, Dodd R, Li Y *et al.* Current and future implications of basic and translational research on amyloid-β peptide production and removal pathways. *Mol Cell Neurosci* 2015; **66**: 3–11.
6 Chapuis J, Hansmannel F, Gistelinck M, Mounier A, Van Cauwenberghe C, Kolen K V *et al.* Increased expression of BIN1 mediates Alzheimer genetic risk by modulating tau pathology. *Mol Psychiatry* 2013; **18**: 1225–1234.
7 Jun G, Ibrahim-Verbaas CA, Vronskaya M, Lambert J-C, Chung J, Naj AC *et al.* A novel Alzheimer disease locus located near the gene encoding tau protein. *Mol Psychiatry* 2015; **21**: 108–117.
8 Shulman JM. Drosophila and experimental neurology in the post-genomic era. *Exp Neurol* 2015; **274**: 4–13.
9 Wittmann CW, Wszolek MF, Shulman JM, Salvaterra PM, Lewis J, Hutton M *et al.* Tauopathy in Drosophila: neurodegeneration without neurofibrillary tangles. *Science* 2001; **293**: 711–714.
10 Sottejeau Y, Bretteville A, Cantrelle F-X, Malmanche N, Demiautte F, Mendes T *et al.* Tau phosphorylation regulates the interaction between BIN1's SH3 domain and Tau's proline-rich domain. *Acta Neuropathol Commun* 2015; **3**: 58.
11 Hu Y, Flockhart I, Vinayagam A, Bergwitz C, Berger B, Perrimon N *et al.* An integrative approach to ortholog prediction for disease-focused and other functional studies. *BMC Bioinformatics* 2011; **12**: 357.
12 Jackson GR, Wiedau-Pazos M, Sang T-K, Wagle N, Brown CA, Massachi S *et al.* Human wild-type tau interacts with wingless pathway components and produces neurofibrillary pathology in Drosophila. *Neuron* 2002; **34**: 509–519.
13 Chatterjee S, Sang T-K, Lawless GM, Jackson GR. Dissociation of tau toxicity and phosphorylation: role of GSK-3beta, MARK and Cdk5 in a Drosophila model. *Hum Mol Genet* 2009; **18**: 164–177.
14 Grabbe C, Zervas CG, Hunter T, Brown NH, Palmer RH. Focal adhesion kinase is not required for integrin function or viability in Drosophila. *Development* 2004; **131**: 5795–5805.
15 Tsai P-I, Kao H-H, Grabbe C, Lee Y-T, Ghose A, Lai T-T *et al.* Fak56 functions downstream of integrin alphaPS3betanu and suppresses MAPK activation in neuromuscular junction growth. *Neural Dev* 2008; **3**: 26.
16 Palmer RH, Fessler LI, Edeen PT, Madigan SJ, McKeown M, Hunter T. DFak56 is a novel *Drosophila melanogaster* focal adhesion kinase. *J Biol Chem* 1999; **274**: 35621–35629.
17 Steinhilb ML, Dias-Santagata D, Mulkearns EE, Shulman JM, Biernat J, Mandelkow E-M *et al.* S/P and T/P phosphorylation is critical for tau neurotoxicity in Drosophila. *J Neurosci Res* 2007; **85**: 1271–1278.
18 Tsai P-I, Wang M, Kao H-H, Cheng Y-J, Walker JA, Chen R-H *et al.* Neurofibromin mediates FAK signaling in confining synapse growth at Drosophila neuromuscular junctions. *J Neurosci* 2012; **32**: 16971–16981.
19 Macagno JP, Diaz Vera J, Yu Y, MacPherson I, Sandilands E, Palmer R *et al.* FAK acts as a suppressor of RTK-MAP kinase signalling in *Drosophila melanogaster* epithelia and human cancer cells. *PLoS Genet* 2014; **10**: e1004262.
20 Patterson KR, Remmers C, Fu Y, Brooker S, Kanaan NM, Vana L *et al.* Characterization of prefibrillar Tau oligomers in vitro and in Alzheimer disease. *J Biol Chem* 2011; **286**: 23063–23076.
21 Köhler C, Dinekov M, Götz J. Active glycogen synthase kinase-3 and tau pathology-related tyrosine phosphorylation in pR5 human tau transgenic mice. *Neurobiol Aging* 2013; **34**: 1369–1379.
22 Schindowski K, Bretteville A, Leroy K, Bégard S, Brion J-P, Hamdane M *et al.* Alzheimer's disease-like tau neuropathology leads to memory deficits and loss of functional synapses in a novel mutated tau transgenic mouse without any motor deficits. *Am J Pathol* 2006; **169**: 599–616.
23 Shulman JM, Imboywa S, Giagtzoglou N, Powers MP, Hu Y, Devenport D *et al.* Functional screening in Drosophila identifies Alzheimer's disease susceptibility genes and implicates Tau-mediated mechanisms. *Hum Mol Genet* 2014; **23**: 870–877.
24 Wang X, Lopez OL, Sweet RA, Becker JT, DeKosky ST, Barmada MM *et al.* Genetic determinants of disease progression in Alzheimer's disease. *J Alzheimers Dis* 2015; **43**: 649–655.
25 Chan G, White CC, Winn PA, Cimpean M, Replogle JM, Glick LR *et al.* CD33 modulates TREM2: convergence of Alzheimer loci. *Nat Neurosci* 2015; **18**: 1556–1558.
26 Simón AM, de Maturana RL, Ricobaraza A, Escribano L, Schiapparelli L, Cuadrado-Tejedor M *et al.* Early changes in hippocampal Eph receptors precede the onset of memory decline in mouse models of Alzheimer's disease. *J Alzheimers Dis* 2009; **17**: 773–786.
27 Mo Y, Williams C, Miller CA. DENN/MADD/IG20 alternative splicing changes and cell death in Alzheimer's disease. *J Mol Neurosci* 2012; **48**: 97–110.

28 Del Villar K, Miller CA. Down-regulation of DENN/MADD, a TNF receptor binding protein, correlates with neuronal cell death in Alzheimer's disease brain and hippocampal neurons. *Proc Natl Acad Sci USA* 2004; **101**: 4210–4215.
29 Steinberg S, Stefansson H, Jonsson T, Johannsdottir H, Ingason A, Helgason H *et al.* Loss-of-function variants in ABCA7 confer risk of Alzheimer's disease. *Nat Genet* 2015; **47**: 445–447.
30 Spillantini MG, Goedert M. Tau pathology and neurodegeneration. *Lancet Neurol* 2013; **12**: 609–622.
31 Kinoshita Y, Hunter RG, Gray JD, Mesias R, McEwen BS, Benson DL *et al.* Role for NUP62 depletion and PYK2 redistribution in dendritic retraction resulting from chronic stress. *Proc Natl Acad Sci USA* 2014; **111**: 16130–16135.
32 Tikhmyanova N, Little JL, Golemis EA. CAS proteins in normal and pathological cell growth control. *Cell Mol Life Sci* 2010; **67**: 1025–1048.
33 Gelman IH. Pyk 2 FAKs, any two FAKs. *Cell Biol Int* 2003; **27**: 507–510.
34 Beck TN, Nicolas E, Kopp MC, Golemis EA. Adaptors for disorders of the brain? the cancer signaling proteins NEDD9, CASS4, and PTK2B in Alzheimer's disease. *Oncoscience* 2014; **1**: 486–503.
35 Bourgin C, Murai KK, Richter M, Pasquale EB. The EphA4 receptor regulates dendritic spine remodeling by affecting beta1-integrin signaling pathways. *J Cell Biol* 2007; **178**: 1295–1307.
36 Parri M, Buricchi F, Giannoni E, Grimaldi G, Mello T, Raugei G *et al.* EphrinA1 activates a Src/focal adhesion kinase-mediated motility response leading to rho-dependent actino/myosin contractility. *J Biol Chem* 2007; **282**: 19619–19628.
37 Williamson R, Scales T, Clark BR, Gibb G, Reynolds CH, Kellie S *et al.* Rapid tyrosine phosphorylation of neuronal proteins including tau and focal adhesion kinase in response to amyloid-beta peptide exposure: involvement of Src family protein kinases. *J Neurosci* 2002; **22**: 10–20.
38 Grace EA, Busciglio J. Aberrant activation of focal adhesion proteins mediates fibrillar amyloid beta-induced neuronal dystrophy. *J Neurosci* 2003; **23**: 493–502.
39 Wright S, Malinin NL, Powell KA, Yednock T, Rydel RE, Griswold-Prenner I. Alpha2beta1 and alphaVbeta1 integrin signaling pathways mediate amyloid-beta-induced neurotoxicity. *Neurobiol Aging* 2007; **28**: 226–237.

Supplementary Information accompanies the paper on the Molecular Psychiatry website (http://www.nature.com/mp)